

NEUTRON DIFFRACTION RESULTS ON THE ORDERING OF AN IRON-CHROMIUM-CARBON AUSTENITE

C. G. Schön*, C. B. R. Parente**, V. L. Mazzocchi** and H. Goldenstein*
*Departamento de Engenharia Metalúrgica e de Materiais da Escola Politécnica
da Universidade de São Paulo, 05508-900 São Paulo-SP, Brasil
**Instituto de Pesquisas Energéticas e Nucleares- IPEN/CNEN-SP, CP 11049
Pinheiros, 05422-970 São Paulo-SP, Brasil.

(Received May 31, 1994)
(Revised July 15, 1994)

Introduction

Order on Fe-Cr-C austenites was first demonstrated by Arbuzov, Golub and Karpets (1), who observed extra reflections in single crystal X-ray diffraction experiments. The reflections were attributed to an Fe₇Cr, face centered cubic superlattice (Space Group: Fm3m) with lattice parameter $a_s = 0.7200$ nm. These results were obtained in alloys within a broad range of compositions (6-10wt%Cr and 0.8-1.2wt%C) and confirmed in the martensite produced after liquid nitrogen quenching of the samples (2). The maximum relative superlattice reflection intensities were found in an Fe-8wt%Cr-1.2wt%C alloy, solubilized at 1473K (1). The ordering of carbon could not be assured from the X-ray diffraction data due to experimental limitations of the technique (1,2), but the authors argue that some kind of "short-range ordering" of carbon in the neighborhood of chromium should be expected due to thermodynamic considerations (2).

In a previous paper by some of the authors (3), the results of a conversion electron Mössbauer spectroscopy (CEMS) experiment in a Fe-8wt%Cr-1.2wt%C austenite was interpreted as evidence of interstitial ordering, with most carbon atoms having at least one chromium atom as near neighbor. The Mössbauer measurements, however, were not sufficient to evaluate the detailed distribution of both carbon and chromium atoms in the lattice of Fe-Cr-C austenites and a complementary experimental technique was required.

The aim of this work is to further investigate the order structure of the austenite of an iron-chromium-carbon alloy using neutron diffraction and, with the help of the Mössbauer results of (3), to determine whether or not the carbon is also ordered in Fe₇Cr superlattice.

Experimental

A Fe-8wt%Cr-1.2wt%C alloy (nominal composition) was prepared and solubilized at 1473K/200h using the procedure described in (3). The as-solubilized sample was submitted to metallographical and X-ray diffraction analysis in order to assure the homogeneity of the microstructure. A cylindrical sample with ~15mm diameter and ~30mm height was taken from the solubilized material and used in the neutron diffraction experiments.

The IPEN neutron diffractometer is a multipurpose instrument installed at the IEA-R1 research reactor. It is a single detector instrument with a fixed angle monochromator. Current wavelength is 0.1133 nm. The acquisition times were varied to maintain a constant transmitted beam intensity of 65,000 counts, resulting in approximately 25 minutes per point. The spectrum was acquired in the interval $10^\circ \leq 2\theta \leq 68^\circ$ with a 0.1° step size.

The DBWS program (4) was used for the Rietveld analysis of the diffraction data. The model used for refining was taken from ref.(1): Iron atoms occupy the positions $4b(1/2,1/2,1/2)$ and $24d(1/4,1/4,0)$, carbon occupy a highly defective interstitial sublattice in positions $8c(1/4,1/4,1/4)$ and $24e(0,0,0.250)$ and the $4a(0,0,0)$ positions have a mixed iron-chromium occupancy. The initial lattice parameter was calculated using the relation $a_\gamma = 2a_\alpha$ (1), where a_γ is the lattice parameter obtained in an X-ray diffraction experiment. The reflections were modeled using a gaussian line profile. The lattice parameter and the isotropic temperature factor (B_{iso}) were refined. The goodness of the fit was measured by the reliability factors, R and R_{wp} defined as:

$$R = \frac{\sum_i |y_i(\text{obs}) - y_i(\text{calc})|}{\sum_i y_i(\text{obs})} \quad R_{wp} = \left\{ \frac{\sum_i w_i^2 \cdot [y_i(\text{obs}) - y_i(\text{calc})]^2}{\sum_i w_i^2 \cdot y_i(\text{obs})^2} \right\}^{1/2} \quad (1)$$

where $y_i(\text{obs})$, $y_i(\text{calc})$ are the observed and calculated intensities and w_i is a weight factor, inversely proportional to the statistical error of the measure. The sum runs over all measured points.

The defect structure of the as-solubilized sample was investigated using a Jeol 2000FX scanning-transmission electron microscope, operating at 200kV. A thin slice ($\sim 500\mu\text{m}$) of the neutron diffraction sample was thinned using the twin-jet electrolytic thinning technique. The electrolyte proposed by Sandvik and Wayman (5) was used, since it operates above the M_s temperature of the alloy.

Results

Chemical analysis of the material resulted in 7.55wt%Cr and 1.14wt%C, with impurity contents less than 0.05wt% except for 0.2wt% aluminum. Based on this composition, the atomic fractions of chromium in the $4a$ positions and of carbon in the interstitial positions were calculated as 65.3% and 5.32% respectively. After solubilization, the microstructure was found to be free from macroscopic inhomogeneities. The X-ray lattice parameter of the austenite was determined as $a_\gamma = 0.3607 \pm 0.004$ nm.

The neutron powder diffraction pattern and the corresponding Rietveld fit (solid line) are shown in Fig. 1. The refined parameters are: $a_\gamma = 0.7192$ and $B_{iso} = 5.9 \cdot 10^{-1} \text{ nm}^2$. The occupancies of the equipoints were not fitted, since an attempt to refine this parameter yielded a departure from the alloy composition. An attempt to introduce carbon atoms preferentially either in the $8c$ or in the $24e$ positions lead to an increase both of R and R_{wp} parameters. The coordinate "z" of position $24e$ could not be refined due to a lack of convergence, it was fixed thus to Arbutov's value $z=0.250$ (1). It was observed that the fit is not too much sensitive to the model chosen for the carbon occupancy. The reliability factors are sufficiently low ($R=6.12\%$ and $R_{wp}=8.39\%$) to imply a good fit. Some discrepancies between the refined and

experimental high angle tails of reflections 222 and 444 were found. The nature of these discrepancies will be discussed later on in this work.

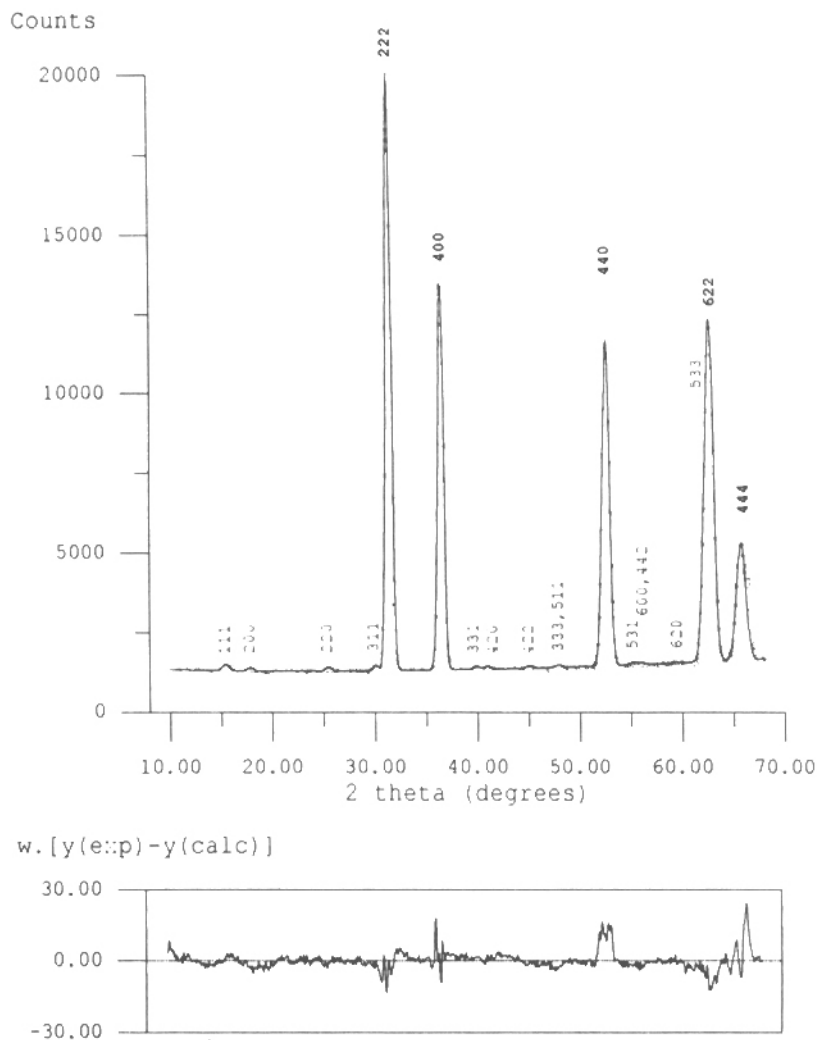


Fig. 1 Neutron diffraction pattern and corresponding difference pattern of the Fe-8wt%Cr-1.2wt%C austenite. The indexes in bold correspond to the principal reflections.

Figures 2a and b present, respectively, an electron micrograph of the sample and its corresponding diffraction pattern. The beam direction was determined to be parallel to the $\langle 01\bar{1} \rangle$ of austenite. A series of long planar features is seen in Fig. 2a. These features are regularly distributed over all the thin area of the sample and are identified as stacking faults by the (111) habit. The use of neutron diffraction allowed us to observe the weak superlattice lines characteristic of the Fe_7Cr phase. A better signal-to-noise ratio of the pattern could only be obtained using isotopical substitution of chromium as in ref.(6). This is because the ^{53}Cr isotope, abundant in natural chromium, increases the nuclear incoherent cross section of the sample by spin incoherent scattering (6).

Discussion

The use of neutron diffraction allowed us to observe the weak superlattice lines characteristic of the Fe₇Cr phase. A better signal-to-noise ratio of the pattern could only be obtained using isotopical substitution of chromium as in ref. (6). This is because the ⁵³Cr isotope, abundant in natural chromium, increases the nuclear incoherent cross section of the sample by spin incoherent scattering (6).

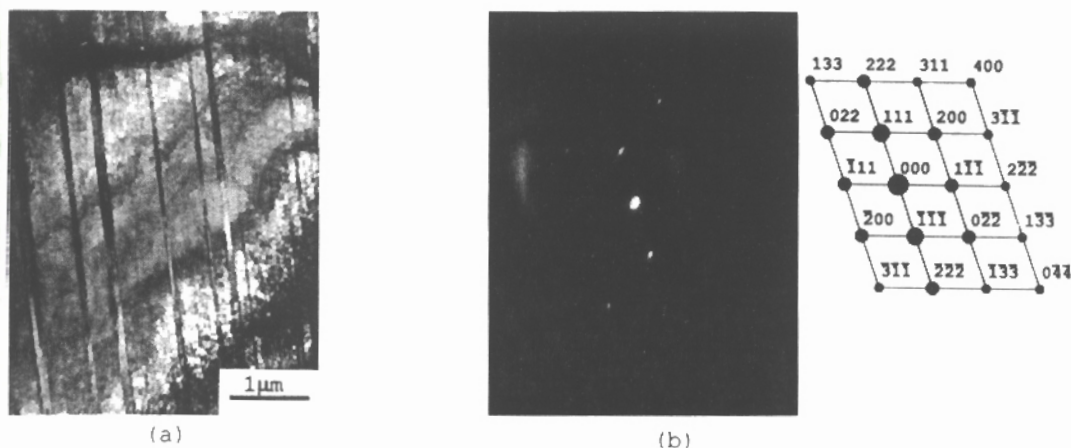


Fig. 2- Bright-field electron image (a) and the corresponding electron diffraction pattern of the austenite (b). The indexes in (b) refer to that of the disordered phase. The corresponding indexes of the superlattice can be found multiplying them by two.

Figure 3 shows schematically the Fe₇Cr superlattice with the octahedral interstices omitted to improve the readability, but the 8c and 24e positions are placed respectively in the centers and on the edges of the eight original FCC cells. The 8c interstices have only iron atoms as near neighbours, while the 24e interstices have one chromium and five iron atoms. Both positions, however, allow configurations where iron atoms have two or more carbon near neighbors, in disagreement with the Mössbauer results of ref. (3). The lack of convergence of the position parameter of equipoint 24e and the fact that no preferential occupation of the neighborhood of chromium by carbon atoms was found in the refining of the neutron data are in contradiction to the same Mössbauer results. This is another evidence of the need for improvement of the interstitials distribution model.

Figures 4a and 4b present details of the neutron diffraction pattern in the region of the 222 and 444 reflections. In Fig. 4a, a deformation of the line is evident, with the high-angle tail decreasing slower than the expected gaussian profile (solid line). The feature associated with the 444 line is more prominent and is resolved as a second peak in the high angle side. Two gaussians were adjusted to the profile of the 444 reflection (dashed and dot-dashed lines in Fig. 4b) and the results are presented in table I. The results show that the intensities of the two peaks support approximately a 2:1 relationship.

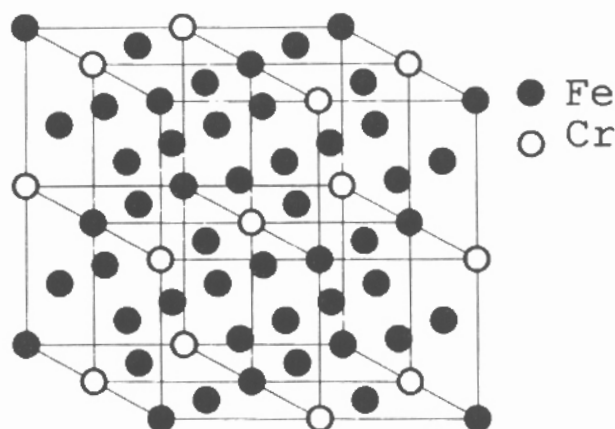


Fig. 3 Unit cell of Fe_7Cr superlattice. The positions occupied by carbon atoms are not shown in order to improve the readability (see text).

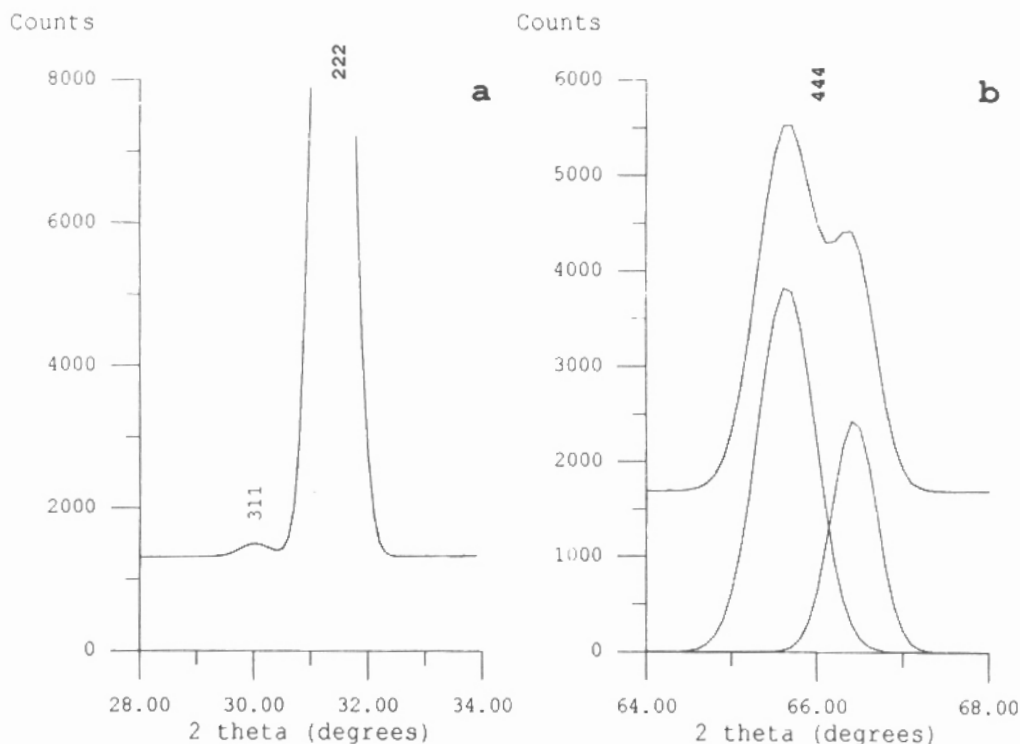


Fig 4 Details from the neutron diffraction pattern near the 222 (a) and 444 (b) reflections. The parameters for the left and right gaussians in figure 4b can be found in table I.

The origin of these features is assumed to be the regularly spaced array of stacking faults observed by TEM (Fig. 2a). In fact, Schwartz and Cohen (9) have shown that the expected effect of stacking faults on powder patterns should be the elongation of the high angle side tail of the 111 reflections (222 in case of the Fe_7Cr superlattice).

TABLE I. Parameters for the Left and Right Adjusted Gaussians of figure 4b.

$y_i = I_i \cdot \exp \left[-\frac{(2\theta_i - 2\theta_k)^2}{2(\Delta 2\theta_k)^2} \right]$			
Gaussian	I_k (counts)	$2\theta_k$ (degrees)	$\Delta 2\theta_k$ (degrees)
left	3847±42	65.640±0.008	0.335±0.006
right	2442±44	66.429±0.009	0.261±0.007

Conclusions

The results obtained in this work confirm the ordering of the Fe-8wt%Cr-1.2wt%C austenite. The distribution of chromium in the ordered austenite agrees with the Fe₇Cr superlattice model proposed by Arbuzov et al(1).

Concerning the carbon distribution, the neutron diffraction data provided no evidence of enrichment of the neighborhood of chromium with carbon atoms, in disagreement with the Mössbauer result of ref. (3), suggesting that the carbon distribution model in the Fe₇Cr superlattice should be improved.

Acknowledgments

This work was supported by Fundação de Amparo à Pesquisa do Estado de São Paulo (FAPESP)- Brasil, under grants 91/4117-9 and 92/4838-0 and by the International Atomic Energy Agency (IAEA) under research contract no. 6974/RB. The authors would like to thank Prof. Dr. L. H. de Almeida and Prof. Dr. G. A. Soares of the PEMM/COPPE- Universidade Federal do Rio de Janeiro, Brasil, for the assistance with the TEM experiments.

References

1. M. P. Arbuzov, S. Ya. Golub and M. V. Karpets, Fiz. Metal. Metalloved. 62, 108 (1986).
2. S. Ya. Golub and M. V. Karpets, Fiz. Metal. Metalloved. 64, 775 (1987).
3. C. G. Schön, H. Rechenberg and H. Goldenstein, Scripta Met. Mater. 29, 1483 (1993).
4. A. Sakthivel and R. A. Young, "User's guide to programs DBWS-9006 and DBWS-9006PC for Rietveld refining of X-ray and neutron powder diffraction patterns", Georgia Inst. of Technology, Atlanta, 1992.
5. Sandvik, B. J. P. and Wayman, C. M., Met. Trans 14A, 2455 (1983).
6. P. Canedesse, F. Fley and S. LeFebvre, Acta Cryst. A40, 228 (1984).
7. O. N. C. Uwakweh, J. Ph. Bauer and J.-M. R. Génin, Met. Trans. 21A, 589 (1990).
8. L. H. Schwartz and J. B. Cohen, "Diffraction from Materials" p. 393, 2nd. Ed., Springer-Verlag, Berlin (1987)